



Short communication

# Electrospun nanofibrous blend membranes for fuel cell electrolytes

Ryouhei Takemori, Hiroyoshi Kawakami\*

Department of Applied Chemistry, Tokyo Metropolitan University, Hachioji, Tokyo 192-0397, Japan

## ARTICLE INFO

## Article history:

Received 5 October 2009  
 Received in revised form  
 29 December 2009  
 Accepted 6 January 2010  
 Available online 14 January 2010

## Keywords:

Nanofiber  
 Sulfonated copolyimide  
 Blend membrane  
 Fuel cell  
 Proton conductivity

## ABSTRACT

We have synthesized the novel blend membranes composed of sulfonated polyimide nanofibers and sulfonated polyimide for proton exchange membrane fuel cell. The proton conductivities of the blend membrane containing nanofibers were measured as functions of the relative humidity and temperature using electrochemical impedance spectroscopy. The proton conductivity of the blend membrane indicated a higher value when compared to that determined for the blend membrane without nanofibers prepared with conventional solvent-casting method. In addition, the membrane stability, such as oxidative and hydrolytic stabilities, of the blend membrane containing nanofibers strongly depended on the amount of nanofiber and was significantly improved with an increase in nanofiber. Oxygen permeability of the membrane was also investigated under dry condition at 35 °C and 760 mm Hg. Oxygen permeability coefficient of the blend membrane slightly decreased when compared to that determined in the blend membrane without nanofibers. Consequently, nanofibers proved to be promising materials as a proton exchange membrane and the blend membrane containing nanofibers may have potential application for use in fuel cells.

© 2010 Elsevier B.V. All rights reserved.

## 1. Introduction

The proton exchange membrane fuel cell converts chemical energy directly into electrical energy with a high efficiency and low emission of pollutants. The proton exchange membrane is one of the key components in fuel cell systems [1,2]. To improve the power density and efficiency of polymer electrolyte membrane, the polymers with high proton conductivity and low gas permeability or cross-over are desired. In addition, the polymer membranes are required to achieve a sufficient thermal stability and long-term durability. The perfluorosulfonated membranes such as Nafion have been widely used because of their excellent oxidative and chemical stability as well as high proton conductivity [3,4]. However, there are several drawbacks of Nafion, such as high cost, low thermal stability, and high gas permeability. Recently, numerous research efforts are focusing on the development of novel polymer electrolyte membranes based on the sulfonated aromatic hydrocarbon polymers, which have been widely synthesized as alternate candidates due to their excellent chemical and thermal stabilities, and good mechanical strength [5–10]. However, most of them contain a large number of sulfonic acid groups to enhance the proton conductivity, resulting in an unfavorable swelling of the membranes and a dramatic loss in their mechanical properties.

Recently, nanofibers prepared by electrospinning have received a lot of attention [11–15]. Electrospinning is capable of producing fibers with diameters in the nanometer range, and the electrospun nanofibers possess many unique properties including a large specific surface area, superior mechanical properties, and use as nanoscale building blocks. However, there are only a few reports in the literature on the proton conductivity of electrospun nanofibrous mats [16–18]. Here, we describe the novel blend membranes composed of sulfonated polyimide nanofibers and sulfonated polyimide for proton exchange membrane fuel cell, which revealed an enhanced proton conductivity, lower gas permeability, and good membrane stability.

## 2. Experimental

### 2.1. Materials

1,4,5,8-Naphthalene tetracarboxylic dianhydride (NTDA) was purchased from the Sigma–Aldrich Co., Tokyo, Japan. 4,4'-Diaminobiphenyl-2,2'-disulfonic acid (BDSA) was purchased from the Tokyo Kasei Co., Tokyo, Japan, and was purified by dissolution in a triethylamine aqueous solution and then precipitated in 1N H<sub>2</sub>SO<sub>4</sub>. Finally, the BDSA was dried in a vacuum oven at 70 °C for 12 h. 2,2-Bis[4-(4-aminophenoxy)phenyl]-hexafluoropropane (APPF) was purchased from the Wako Pure Chemical Industries Co., Osaka, Japan, and then was recrystallized twice from an ethanol solution prior to use. Nafion® 117 was used in this study as the control membrane. The membranes were obtained from the DuPont Co., Ltd. (Tokyo, Japan).

\* Corresponding author. Tel.: +81 426 77 1111x4972; fax: +81 426 77 2821.  
 E-mail address: [kawakami-hiroyoshi@cm.metro-u.ac.jp](mailto:kawakami-hiroyoshi@cm.metro-u.ac.jp) (H. Kawakami).

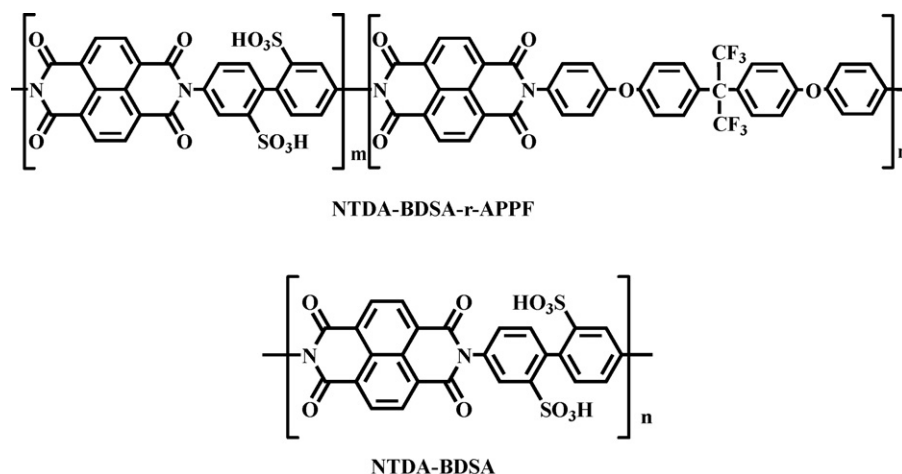


Fig. 1. Chemical structure of sulfonated polyimide.

## 2.2. Syntheses of sulfonated polyimides

The sulfonated random copolyimide, NTDA-BDSA-r-APPF, and the sulfonated polyimide, NTDA-BDSA, were synthesized by the same method as described in previous papers (Fig. 1) [9,10]. The molar ratio of BDSA to APPF was set at 1:1. The molecular weights ( $M_w$  and  $M_n$ ) of the oligomers and sulfonated copolyimides were determined by gel-permeation chromatography (detector: Jasco 830-RI monitor) using two Shodex SB-806HQ and SB-804 HQ columns. Dimethylformamide containing 0.01 M lithium bromide was used as the eluent at a flow rate of  $1.0 \text{ ml min}^{-1}$ . The molecular weights were estimated by comparing the retention times on the columns to those of standard polystyrene. The ionic-exchange capacity (IEC) was measured by classical titration using NaOH and HCl solutions [9,10].

## 2.3. Preparation of blend membrane containing nanofibers

The experimental set-up used for the preparation of the non-woven nanofibers is shown in Fig. 2 [11]. The nanofibers were fabricated using an electrospinning apparatus (Fucec, Co., Ltd., ES-1000, Tokyo, Japan).

NTDA-BDSA-r-APPF was dissolved in DMF. The typical electrospinning parameters were as follows: the polymer solution with

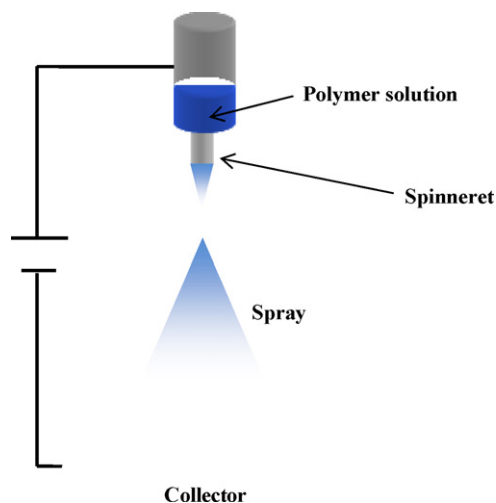


Fig. 2. Schematic diagram of electrospinning apparatus.

a 15 wt% concentration was loaded into a 1 ml syringe as the spinneret. A syringe pump was used to squeeze out the polymer solution at the speed of  $0.12 \text{ ml h}^{-1}$  through a needle with an inner diameter of 0.21 mm. A voltage of 30 kV was applied between the syringe and the collector. The distance between the spinneret and the grounded plate was 10 cm. To remove the residual solvent from the fabricated non-woven nanofibers, vacuum drying was carried out at  $150^\circ\text{C}$  for 10 h. In addition, the NTDA-BDSA-r-APPF nanofibers were acidified with HCl solution for 24 h. Then the sulfonated polyimide, NTDA-BDSA, solution was poured to the nanofibers, and the mixture solution was dried in a vacuum oven at  $110^\circ\text{C}$  for 24 h. After drying, the blend membrane containing non-woven NTDA-BDSA-r-APPF nanofibers was acidified with 0.1 M HCl solution for 24 h, and finally washed with deionized water. The resulting membrane was dried in a vacuum oven at  $80^\circ\text{C}$  for 24 h. The thickness of the membrane was approximately  $50 \mu\text{m}$ . The nanofibers were observed using a scanning electron microscope (SEM, JXP-6100P, JEOL, Tokyo, Japan).

## 2.4. Characterization of membrane

The water uptake of the blend membrane containing nanofibers was gravimetrically measured from the dried and humidified membranes [9,10]. The membranes were dried in a vacuum oven at  $80^\circ\text{C}$  for 10 h and then immersed in liquid water at room temperature. After 24 h, the membrane was then wiped dry and quickly weighed. The water uptake was calculated using Eq. (1)

$$W(\%) = \frac{W_s - W_d}{W_d} \times 100 \quad (1)$$

where  $W_s$  is the weight of the membrane in the swollen state and  $W_d$  is the weight of the membrane in the dry state.

The stability of the blend membranes containing nanofibers to oxidation was investigated by immersing the membranes ( $1 \text{ cm} \times 1 \text{ cm}$ ) in Fenton's reagent (30 ppm  $\text{FeSO}_4$  in 30%  $\text{H}_2\text{O}_2$ ) at  $80^\circ\text{C}$ . The hydrolytic stability of the membranes ( $1 \text{ cm} \times 1 \text{ cm}$ ) was performed by immersing that into deionized water at  $80^\circ\text{C}$  and the stability was characterized by the time that the membrane was dissolved completely. The thickness of the membranes was approximately 50 mm. The membranes for both measurements were stirred in Fenton's reagent or deionized water.

## 2.5. Proton conductivity of membrane

The proton conductivity of the blend membranes containing nanofibers was measured by electrochemical impedance spec-

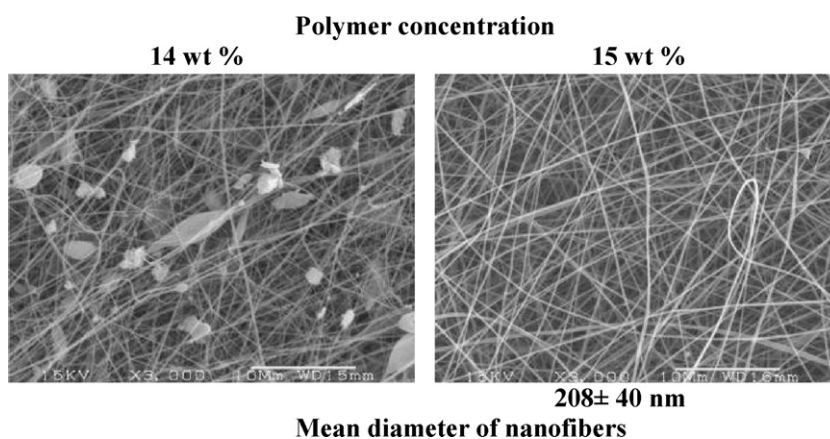


**Fig. 3.** SEM images of NTDA-BDSA-r-APPF nanofibers electrospun on collector.

troscopy over the frequency range from 50 Hz to 50 kHz (Hioki 3532-50, Tokyo, Japan) as reported in previous papers [9,10]. The blend membranes (1.0 cm × 3.0 cm) and two blackened platinum plate electrodes were placed in a Teflon cell. The distance between the two electrodes was 1.0 cm. The cell was placed in a thermo-controlled humidity chamber to measure the temperature and humidity dependence of the proton conductivity.

### 3. Results and discussion

#### 3.1. Preparation of NTDA-BDSA-r-APPF nanofiber

The sulfonated random copolyimide, NTDA-BDSA-r-APPF, and sulfonated polyimide, NTDA-BDSA, were synthesized by chemical imidization from the precursor as reported in previous papers [9,10]. The poly(amic acid) polyimides were converted to the polyimide by chemical imidization and the molecular weights of the polyimides were determined by gel-permeation chromatography. The molecular weight of NTDA-BDSA-r-APPF and NTDA-BDSA was  $2.8 \times 10^5$  and  $7.2 \times 10^5$ , respectively.

The electrospinning process is a method of discharging a polymer solution in air from a nozzle under high voltage and producing a nanofiber by exploiting electrostatic repulsion of the polymer solution. It has been reported that the shape of the initiating droplet through the spinneret can be changed by the electrospinning conditions such as applied voltage, viscosity and feed rate of the polymer solution, and the distance between the spinneret and the grounded plate as collector. In particular, significant morphological changes were found when the concentration or viscosity of the polymer solution was changed, which means that the concentration or viscosity of the polymer solution was one of the most effective variables to control the nanofiber morphology. We found that it is impossible to fabricate a continuous nanofiber at a concentration of NTDA-BDSA-r-APPF dissolved in DMF below 14 wt%. It

was found that the nanofibers electrospun at concentrations below 14 wt% were composed of a mixture of fibers and beads.

Fig. 3 is SEM images of NTDA-BDSA-r-APPF nanofibers on a grounded aluminum plate. The applied voltage was 30 kV, and the feeding and the concentration of the polymer solution were  $0.12 \text{ ml h}^{-1}$  and 15 wt%, respectively. The distance between the spinneret and the grounded plate was 10 cm. The images showed that the nanofibers had a uniform fiber-diameter, however, they were randomly aligned on the plate. The mean diameter of the nanofibers was  $208 \pm 40 \text{ nm}$  ( $n = 25$ ).

#### 3.2. Proton conductivity of blend membrane containing nanofibers

The proton conductivities of the blend membrane containing non-woven nanofibers were measured as a function of the temperature and relative humidity. The blend membrane with the different nanofiber contents was prepared as mentioned above. The blend membrane without nanofiber, which was prepared from NTDA-BDSA-r-APPF and NTDA-BDSA solutions, was used as control membrane for the blend membrane with nanofiber.

Table 1 shows the effect of the amount of nanofiber on the proton conductivity of the blend membranes. The proton conductivity of NTDA-BDSA membrane indicated the largest value in all the membranes due to the highest IEC, while that of NTDA-BDSA-r-APPF was the smallest due to the lowest one. On the other hand, for comparison the blend membrane (2) with the blend membrane, which is prepared from the ratio of NTDA-BDSA/NTDA-BDSA-r-APPF = 80/20, the proton conductivities of the blend membrane (2) were significantly superior to those measured in the blend membrane. The tendency of the proton conductivity was in particular remarkable at low temperature or low humidity. In most polymer electrolyte membranes, the proton conductivities of the membranes are strongly related to the amount of sulfonic acid groups

**Table 1**

IEC values, water uptakes, and proton conductivities of blend membranes.

Membrane	Weight ratio (%) NTDA-BDSA:NTDA-BDSA-r-APPF	IEC (mequiv. g <sup>-1</sup> )	Water uptake (%)	Proton conductivity (S cm <sup>-1</sup> )		
				98% RH		30% RH
				30 °C	80 °C	80 °C
NTDA-BDSA	100:0	3.0	72	$8.2 \times 10^{-2}$	$5.9 \times 10^{-1}$	$4.4 \times 10^{-4}$
NTDA-BDSA-r-APPF	0:100	1.5	33	$7.0 \times 10^{-3}$	$5.6 \times 10^{-2}$	$6.8 \times 10^{-5}$
Blend membrane	80:20	2.7	55	$1.8 \times 10^{-2}$	$2.3 \times 10^{-1}$	$9.4 \times 10^{-5}$
Blend membrane (1)	90:10	2.8	60	$5.5 \times 10^{-2}$	$3.7 \times 10^{-1}$	$2.2 \times 10^{-4}$
Blend membrane (2)	80:20	2.7	53	$5.0 \times 10^{-2}$	$3.3 \times 10^{-1}$	$1.8 \times 10^{-4}$
Blend membrane (3)	70:30	2.6	43	$3.8 \times 10^{-2}$	$2.1 \times 10^{-1}$	$1.3 \times 10^{-4}$

Blend membranes (1), (2) and (3) are composed of NTDA-BDSA membrane and NTDA-BDSA-r-APPF nanofibers.

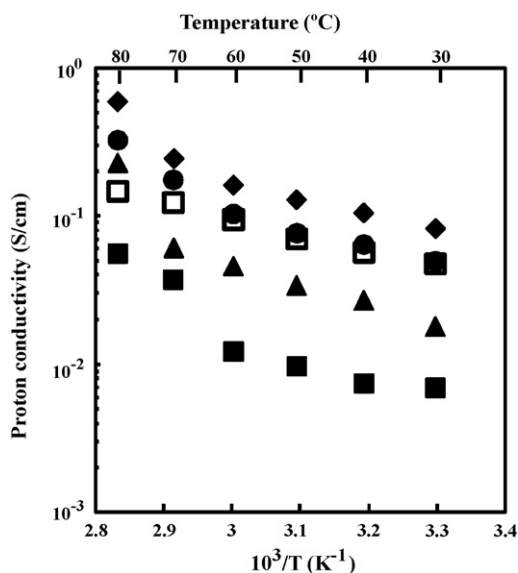


Fig. 4. Temperature dependence of proton conductivity for blend membranes at 98%RH: (◆) NTDA-BDSA; (■) NTDA-BDSA-r-APPF; (▲) blend membrane; (●) blend membrane (2); (□) Nafion 117.

or the water content of the membrane, and polymer electrolyte membranes absorbing a large amount of water typically have a high proton conductivity. Therefore, generally, there is good correlation between proton conductivity and IEC or water uptake. However, as shown in Table 1, those values of the blend membrane (2) and the blend membrane without nanofiber are almost constant, therefore, we think that ionic channel formed in nanofiber and that the protons were rapidly and efficiently transported in nanofiber. On the other hand, the proton conductivity of the blend membrane containing nanofibers strongly depended on the amount of nanofiber and decreased with an increase in nanofiber because of addition of NTDA-BDSA-r-APPF with low proton conductivity.

Fig. 4 shows the temperature dependence of the proton conductivity of the membrane at 98% relative humidity. It was found that the blend membrane (2) showed higher proton conductivity when compared with the blend membrane without nanofibers and Nafion, at all temperatures.

Fig. 5 shows the relative humidity dependence of the proton conductivity for the membranes at 80 °C. The blend membrane (2) showed conductivity comparable to that of Nafion at high humidity and high temperature. At lower humidity, however, the proton conductivity decreased down to the order of  $10^{-4}$  S  $\text{cm}^{-1}$ . This is the behavior often observed for the sulfonated aromatic hydrocarbon polymers. On the other hand, the blend membrane (2) indicated higher values than the blend membrane without nanofiber at low humidity.

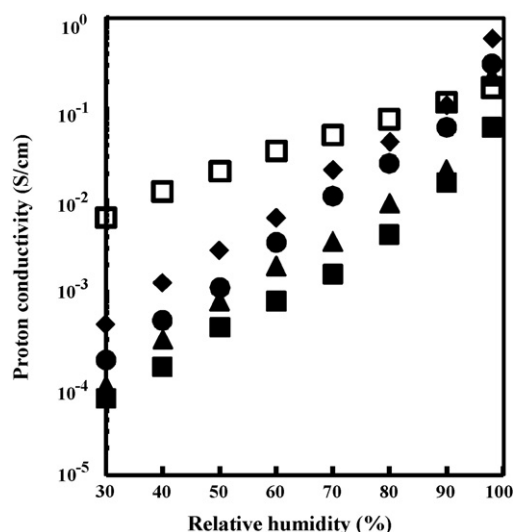


Fig. 5. Relative humidity dependence of proton conductivity for blend membranes at 80 °C: (◆) NTDA-BDSA; (■) NTDA-BDSA-r-APPF; (▲) blend membrane; (●) blend membrane (2); (□) Nafion 117.

### 3.3. Membrane stability and gas permeability of blend membrane

Generally, most of the membranes contain a large number of sulfonic acid groups to enhance the proton conductivity, resulting in an unfavorable swelling of the membranes and a dramatic loss in their mechanical properties. Therefore, membrane stability plays a very important role in the properties of the proton exchange membranes. In this study, the oxidative and hydrolytic stabilities of the blend membranes were evaluated in Fenton's reagent and water at 80 °C, as shown in Table 2. The NTDA-BDSA-r-APPF membrane with low IEC showed relatively good resistance to the oxidation and hydrolytic degradations. On the other hand, the NTDA-BDSA membrane with high IEC was dissolved for 1 h for both measurements. For comparison the blend membrane (2) with the blend membrane, the blend membrane (2) indicated relative excellent membrane stability. These findings indicate that the blend membranes containing the nanofibers have good stability for the oxidation and hydrolytic degradations. In addition, the membrane stability of the nanofibrous blend membrane strongly depended on the amount of nanofiber and was significantly improved with an increase in nanofiber. Particularly, the blend membrane (3) endured 500 h for hydrolytic measurement and kept its toughness after the measurement. Recently, orientation of polymer chains at molecular level within nanofibers was elucidated using polarized Fourier transform infrared spectroscopy, polarized Raman spectroscopy, and wide-angle X-ray diffraction [19,20]. We consider that the oriented and ordered molecular architecture in nanofibers may have influence on the membrane stability. Therefore, it should be noted

Table 2  
Oxidative stability, hydrolytic stability, and oxygen permeability of blend membranes.

Membrane	Oxidative stability <sup>a</sup> (h)	Hydrolytic stability <sup>b</sup> (h)	PO <sub>2</sub> <sup>c</sup> (Barrer)	DO <sub>2</sub> <sup>d</sup>	SO <sub>2</sub> <sup>e</sup>
NTDA-BDSA	0.2	0.5	0.35	0.21	1.7
NTDA-BDSA-r-APPF	10	700	2.4	0.96	2.5
Blend membrane	2.0	144	0.66	0.41	1.6
Blend membrane (1)	1.0	168	0.39	0.35	1.1
Blend membrane (2)	5.0	450	0.52	0.39	1.3
Blend membrane (3)	7.0	600	0.62	0.41	1.5

<sup>a</sup> The oxidative stability (30 ppm FeSO<sub>4</sub> in 30% H<sub>2</sub>O<sub>2</sub>) was characterized by the time that the membranes dissolved completely at 80 °C.

<sup>b</sup> The hydrolytic stability was characterized by the time that the membranes dissolved completely at 80 °C.

<sup>c</sup> At 35 °C and 76 cm Hg. Barrer:  $10^{-10}$  [cm<sup>3</sup> (STP) cm]/(cm<sup>2</sup> s cm Hg)].

<sup>d</sup> D:  $1 \times 10^{-8}$  (cm<sup>2</sup> s<sup>-1</sup>).

<sup>e</sup> S:  $1 \times 10^{-2}$  (cm<sup>3</sup> (STP)/cm<sup>3</sup> cm Hg).

that the introduction of nanofiber into membrane is effectively for the membrane stability. As apparent from Table 2, the values of oxidative and the hydrolytic stabilities for the blend membrane (2) improved more than double when compared to those determined in the blend membrane. However, both stabilities of the nanofibrous blend membranes were not sufficient to use useful materials for fuel cell electrolytes yet due to poor stability of NTDA–BDSA used in this study. With future research, we will prepare the electrospun nanofibrous blend membranes composed of the sulfonated polyimide with good membrane stability.

Gas permeability of the membrane is another important factor that affects fuel cell performance, because the permeated hydrogen or oxygen causes direct chemical reaction combustion resulting in lower utilization of fuels and higher overpotential. Oxygen permeability of the membrane was investigated under dry condition at 35 °C and 760 mm Hg, as shown in Table 2. Oxygen permeability coefficient ( $PO_2$ ) of the blend membrane (2) slightly decreased when compared to that determined in the blend membrane, suggesting that the introduction of nanofiber into the proton exchange membrane suppresses the gas permeability. This is because the oriented and ordered molecular architecture in nanofibers may have influence on the gas permeability through the polymer membranes. Therefore, it should be noted that the introduction of nanofiber into membrane is also effective for the suppression of gas permeability.

#### 4. Conclusions

Control of the proton conductivity and membrane stability of proton exchange membranes has become a subject of strong research interest. However, many studies of relationships between the proton conductivity and membrane stability of the membranes have led to trade-off correlations, which have become a major problem in realizing proton exchange membranes using polymer materials. We prepared the novel blend membranes containing sulfonated polyimide nanofibers for proton exchange membrane fuel cell and demonstrated that the proton conductivity of the nanofibrous blend membrane indicated a higher value when compared to that determined for the blend membrane without nanofibers prepared with conventional solvent-casting method. In addition,

we demonstrated that the membrane stability, such as oxidative and hydrolytic stabilities, of the nanofibrous blend membrane strongly depended on the amount of nanofiber and was significantly improved with an increase in nanofiber. It should be emphasized here that gas permeability of the membrane containing nanofibers also decreased when compared to that determined in the blend membrane without nanofibers. These findings indicate that such blend membranes containing nanofibers may break trade-off correlations between the proton conductivity and membrane stability prepared of fuel cell electrolyte membranes. We consider that the electrospun nanofibrous blend membranes may prove to be promising materials as polymer electrolyte membranes having high proton conductivity, good membrane stability, and low gas permeability or cross-over and may be potentially useful for application in fuel cells.

#### References

- [1] R.F. Service, *Science* 303 (2004) 29.
- [2] B.C.H. Steele, A. Heinzel, *Nature* 414 (2001) 345.
- [3] N.W. Deluca, Y.A. Elabd, *J. Polym. Sci. Part B: Polym. Phys.* 44 (2006) 2201.
- [4] P. Choi, N.H. Jalani, T.M. Thampan, R. Datta, *J. Polym. Sci. Part B: Polym. Phys.* 44 (2006) 2183.
- [5] M. Guo, B. Liu, Z. Liu, L. Wang, Z. Jiang, *J. Power Sources* 189 (2009) 894.
- [6] J. Saito, K. Miyatake, M. Watanabe, *Macromolecules* 41 (2008) 2415.
- [7] J. Chen, M. Asano, Y. Maekawa, M. Yoshida, *J. Membr. Sci.* 319 (2008) 1.
- [8] J. Parvole, P. Jannasch, *Macromolecules* 41 (2008) 3893.
- [9] Y. Okazaki, S. Nagaoka, H. Kawakami, *J. Polym. Sci. Part B: Polym. Phys.* 45 (2007) 1325.
- [10] T. Nakano, S. Nagaoka, H. Kawakami, *Polym. Adv. Technol.* 16 (2005) 753.
- [11] Y. Karube, H. Kawakami, *Polym. Adv. Technol.* (in press).
- [12] G.Y. Yun, H.S. Kim, J. Kima, K. Kim, C. Yang, *Sens. Actuators A* 141 (2008) 530.
- [13] R. Gopal, S. Kaur, Z. Ma, C. Chan, S. Ramakrishna, T. Matsuura, *J. Membr. Sci.* 281 (2006) 581.
- [14] F. Yang, R. Murugan, S. Wang, S. Ramakrishna, *Biomaterials* 26 (2005) 2603.
- [15] Z. Ma, M. Kotaki, S. Ramakrishna, *J. Membr. Sci.* 265 (2005) 115.
- [16] J. Choi, K.M. Lee, R. Wycisk, P.N. Pintauro, P.T. Mather, *Macromolecules* 41 (2008) 4569.
- [17] A. Laforge, L. Robitaille, A. Mokriani, A. Aji, *Macromol. Mater. Eng.* 292 (2007) 1229.
- [18] X. Li, X. Hao, D. Xu, G. Zhang, S. Zhang, H. Na, D. Wang, *J. Membr. Sci.* 281 (2006) 1.
- [19] T. Kongklang, K. Tashiro, M. Kotaki, S. Chirachanchai, *J. Am. Chem. Soc.* 130 (2008) 15466.
- [20] M.V. Kakade, S. Givens, K. Gardner, K.H. Lee, D.B. Chase, J.F. Rabolt, *J. Am. Chem. Soc.* 129 (2007) 2777.